

Photoinduced Oxidation of Horseradish Peroxidase

Johan Berglund, Torbjörn Pascher, Jay R. Winkler,* and Harry B. Gray*

Contribution from the Beckman Institute, California Institute of Technology,
Pasadena, California 91125

Received March 28, 1996. Revised Manuscript Received August 20, 1996[⊗]

Abstract: Photoexcited $[\text{Ru}(\text{bpy})_3]^{2+}$ ($\text{bpy} = 2,2'$ -bipyridine) can be quenched with $[\text{Co}(\text{NH}_3)_5\text{Cl}]^{2+}$ to give $[\text{Ru}(\text{bpy})_3]^{3+}$; this photogenerated oxidant ($E^0 = 1.25 \text{ V vs NHE}$) reacts with horseradish peroxidase isoenzyme *c* (HRPc) to produce oxidized protein species. Spectra and kinetics measured by laser-flash transient spectroscopy show that oxidation of the trivalent resting state, $[\text{PFe}^{\text{III}}]^+$ ($\text{P} = \text{porphyrin dianion}$), to ferryl compound **II**, $[\text{PFe}^{\text{IV}}=\text{O}]$, is preceded by generation of a π -cation porphyrin radical intermediate, $[\text{PFe}^{\text{III}}]^{2+}$. In the interval $7.8 < \text{pH} < 9.8$, the rate-limiting step for the transformation of the radical intermediate to compound **II** is the binding of a water molecule to the five-coordinate heme iron, $k_{\text{obsd}} = (4.1 \pm 0.9) \text{ s}^{-1}$; this step is followed by fast proton and electron transfer to give the ferryl species. There is a burst in compound **II** formation in the pH region ($10.3 < \text{pH} < 10.8$) in which the heme iron changes from a five-coordinate, high-spin species to a six-coordinate, low-spin complex ($\text{p}K_{\text{a}} = 10.9$); this burst is attributed to very rapid conversion of a hydroxo-ligated ferric π -cation radical porphyrin to a ferryl species. The rate constant for the porphyrin-centered oxidation of compound **II** to compound **I** ($[\text{PFe}^{\text{IV}}=\text{O}]$) to $[\text{PFe}^{\text{IV}}=\text{O}]^{+}$; $k = 1.1 \times 10^8 \text{ M}^{-1} \text{ s}^{-1}$) is slightly larger than that for the oxidation of $[\text{PFe}^{\text{III}}]^+$ to $[\text{PFe}^{\text{III}}]^{2+}$ ($k = 2.5 \times 10^7 \text{ M}^{-1} \text{ s}^{-1}$) at pH 10.3; both porphyrin-centered oxidations are much faster than the conversion of $[\text{PFe}^{\text{III}}]^+$ to $[\text{PFe}^{\text{IV}}=\text{O}]$ below pH 9.8.

Introduction

The ferryl species $[\text{PFe}^{\text{IV}}=\text{O}]$ and $[\text{PFe}^{\text{IV}}=\text{O}]^{+}$ ($\text{P} = \text{porphyrin dianion}$), known as compound **II** and compound **I**, respectively, are the catalytically active intermediates in the catalase and peroxidase cycles.^{1–3} Both species contain a ferryl ion that is one oxidation equivalent above the ferric resting state, but a second oxidation equivalent is stored as a radical in compound **I**, either on an amino-acid residue (cytochrome *c* peroxidase)⁴ or on the porphyrin ring (HRP).^{5,6} The compounds are strong oxidants ($E^0(\text{compound I}/\text{compound II}) = 898 \text{ mV}$ and $E^0(\text{compound II}/\text{ferric}) = 870 \text{ mV vs NHE}$ at $25 \text{ }^\circ\text{C}$ for horseradish peroxidase, HRP)⁷ capable of oxidizing a wide variety of substrates. A compound **I** equivalent also has been postulated as the species that transfers an oxygen atom to substrate in monooxygenases such as cytochrome P-450.^{1,3}

Peroxidase compound **I** can be generated by oxidation of the ferric resting state by hydrogen peroxide or strong one-electron oxidants such as K_2IrCl_6 .^{8–11} Kinetics studies have shown that oxidations of substrates by compound **I** are normally 10 to 1000 times faster than oxidations by compound **II**.^{10–16} This striking difference in reactivity can be rationalized in terms of the

electronic structures of the two oxidized heme compounds. Specifically, electron transfer to the porphyrin radical cation would be expected to be much faster than reduction of ferryl to ferric, because the latter reaction involves coupled proton/electron-transfer steps. It follows that the initial event in the oxidation of the ferric state to compound **II** could be electron transfer from the porphyrin, thereby generating a radical intermediate ($[\text{PFe}^{\text{III}}]^{2+}$) that subsequently would convert to the ferryl form. Such a radical has been observed as a product in the oxidation of zinc, magnesium, and fluoride derivatives of HRP,^{17–19} as well as in porphyrin model complexes,^{20–26} but has eluded detection in native peroxidases.

We have developed a photochemical method for generating ferryl species that permits measurements on significantly faster time scales than can be achieved using conventional stopped-flow spectroscopy. In this approach, strongly oxidizing $[\text{Ru}(\text{bpy})_3]^{3+}$ ($\text{bpy} = 2,2'$ -bipyridine; $E^0(\text{Ru}^{3+}/\text{Ru}^{2+}) = 1.25 \text{ vs NHE}$)²⁷ is produced photochemically by quenching pulsed-laser excited $[\text{Ru}(\text{bpy})_3]^{2+}$ with suitable oxidants ($[\text{Ru}(\text{NH}_3)_6]^{3+}$, $[\text{Co}(\text{NH}_3)_5\text{Cl}]^{2+}$). We have previously used this method to generate both $[\text{PFe}^{\text{III}}]^{2+}$ and compound **II** ($\text{PFe}^{\text{IV}}=\text{O}$) in the heme-containing peptide microperoxidase-8 (MP8) at pH 6.²⁸ In the present study, we have applied this ferryl-generating

[⊗] Abstract published in *Advance ACS Abstracts*, February 15, 1997.
(1) Valentine, J. S. In *Bioinorganic Chemistry*; Bertini, I., Gray, H. B., Lippard, S. J., Valentine, J. S., Eds.; University Science Books: Mill Valley, CA, 1994; pp 253–315.
(2) Dunford, H. B.; Stillman, J. S. *Coord. Chem. Rev.* **1976**, *19*, 187.
(3) Dawson, J. H. *Science* **1988**, *240*, 433.
(4) Erman, J. E.; Vitello, L. B.; Mauro, J. M.; Kraut, J. *Biochemistry* **1989**, *28*, 7992.
(5) Palaniappan, V.; Turner, J. J. *Biol. Chem.* **1989**, *264*, 16046.
(6) Chuang, W.-J.; Van Wart, H. E. *J. Biol. Chem.* **1992**, *267*, 13293.
(7) Farhangrazi, Z. S.; Fossett, M. E.; Powers, L. S.; Ellis, W. R., Jr. *Biochemistry* **1995**, *34*, 2866.
(8) George, P. *Science* **1953**, *117*, 220.
(9) Fergusson, R. R. *J. Am. Chem. Soc.* **1956**, *78*, 741.
(10) Hayashi, Y.; Yamazaki, I. *J. Biol. Chem.* **1979**, *254*, 9101.
(11) Farhangrazi, Z. S.; Copeland, B. R.; Nakayama, T.; Amachi, T.; Yamazaki, I.; Powers, L. S. *Biochemistry* **1994**, *33*, 5647.
(12) Brill, A. S. *Comp. Biochem.* **1966**, *14*, 447.
(13) Hasinoff, B. B.; Dunford, H. B. *Biochemistry* **1970**, *9*, 4930.
(14) Bohne, C.; MacDonald, D. I.; Dunford, H. B. *J. Biol. Chem.* **1987**, *262*, 3572.

(15) Nakamura, M.; Hayashi, T. *Arch. Biochem. Biophys.* **1992**, *299*, 313.
(16) Nakamura, M. *J. Biochem.* **1991**, *110*, 595.
(17) Kaneko, Y.; Tamura, M.; Yamazaki, I. *Biochemistry* **1980**, *19*, 5795.
(18) Kuwahara, Y.; Tamura, M.; Yamazaki, I. *J. Biol. Chem.* **1982**, *257*, 11517.
(19) Farhangrazi, Z. S.; Sinclair, R.; Powers, L.; Yamazaki, I. *Biochemistry* **1995**, *34*, 14970.
(20) Phillippi, M. A.; Shimomura, E. T.; Goff, H. M. *Inorg. Chem.* **1981**, *20*, 1322.
(21) Phillippi, M. A.; Goff, H. M. *J. Am. Chem. Soc.* **1982**, *104*, 6026.
(22) Brault, D.; Neta, P. *J. Phys. Chem.* **1984**, *88*, 2857.
(23) Brault, D.; Neta, P. *Chem. Phys. Lett.* **1985**, *121*, 28.
(24) Marguet, S.; Hapiot, P.; Neta, P. *J. Phys. Chem.* **1994**, *98*, 7136.
(25) Gans, P.; Buisson, G.; Duee, E.; Marchon, J.-C.; Erler, B. S.; Scholz, W. F.; Reed, C. A. *J. Am. Chem. Soc.* **1986**, *108*, 1223.
(26) Groves, J. T.; Gross, Z.; Stern, M. K. *Inorg. Chem.* **1994**, *33*, 5065.
(27) Hoffman, M. Z.; Bolleta, F.; Moggi, L.; Hug, G. L. *J. Phys. Chem. Ref. Data* **1989**, *18*, 219–543.

technique to HRP. We have found that the ferric porphyrin π -cation radical again is the initial product of $[\text{PFe}^{\text{III}}]^+$ oxidation, but that the conversion of this species to the ferryl form is much slower than in MP8. As with oxidation by K_2IrCl_6 ,¹⁰ the oxidation of compound **II** to compound **I** by $[\text{Ru}(\text{bpy})_3]^{3+}$ is significantly faster than the conversion of the ferric state to compound **II**.

Experimental Section

Materials. Horseradish peroxidase isoenzyme *c*, HRPc, was obtained by purification of HRP Type I or Type II from Sigma by CM and DEAE cellulose column chromatography according to the method described by Shannon et al.²⁹ An R_z -value (A_{403}/A_{280}) of 3.4 was determined after the final chromatography on a CM-cellulose column. The concentration of the enzyme stock solution was calculated from the absorption at 403 nm where $\epsilon = 1.02 \times 10^5 \text{ M}^{-1} \text{ cm}^{-1}$.³⁰ $[\text{Ru}(\text{bpy})_3]\text{Cl}_2$ (Strem) and $[\text{Co}(\text{NH}_3)_5\text{Cl}]\text{Cl}_2$ (Aldrich, 99.999%) were used as received. pH was adjusted using either phosphate (pH 7.0–7.8), borate (pH 8.5–9.8), or carbonate (pH 10.3–10.8); the concentration of buffer was between 10 and 100 mM. Since ionic strength ($I < 400 \text{ mM}$) had no influence on the rate of oxidation of $\text{HRPcFe}^{\text{III}}$, no effort was made to adjust it; in our experiments, ionic strength was typically in the range $50 \text{ mM} < I < 200 \text{ mM}$. Water was purified by a Barnstead E-Pure system before use.

Methods. Steady-state spectra were recorded using a Hewlett Packard (HP-8452) diode array spectrophotometer. Kinetics measurements were made at ambient temperature ($\sim 22^\circ\text{C}$) by use of the laser flash photolysis setup previously described.²⁸ All samples were deoxygenated by gentle and repeated evacuation followed by backfilling with purified argon on a vacuum line. The energy per laser pulse was typically 1 mJ, giving roughly $1 \mu\text{M}$ $[\text{Ru}(\text{bpy})_3]^{3+}$ under the present experimental conditions. Mono- and biphasic kinetic traces were evaluated using a least-squares fitting program.³¹ Reported rate constants are average values from at least five kinetics traces. Transient spectra at pH 9.75 were recorded with a setup consisting of a 75-W xenon arc lamp, mounted in an Oriel Photomax lamp housing and powered by a Photon Technology International LPS-220 power supply, and an Analog Modules 778-P current pulser, synchronized with an Uniblitz L32T2 shutter, to give 1-ms probe-light pulses. The timing between the laser and the probe light was controlled by an EG&G Digital delay generator (9650). The probe light was split into two beams, one passing through the sample and one around it. The two beams were dispersed by a spectrograph (Acton Research Corp. SpectraPro-275) and their intensities were measured using a dual diode array detector (Princeton Instruments).

Results and Discussion

Steady-State Photolysis. The different forms of HRP exhibit distinct electronic spectral features in both the Soret and Q-band regions (Figure 1). We have focused mainly on the Soret region where the overall spectral changes for conversion of one form to another are generally much larger than those further to the red. The Soret peak of compound **II** is red-shifted relative to that of the trivalent resting state ($\text{HRPcFe}^{\text{III}}$) but the absorptivities at the maxima are similar.³² The absorptivities of compound **I**, however, are well below those for $\text{HRPcFe}^{\text{III}}$ through most of the Soret region due to the presence of the porphyrin π -cation radical. The broad decrease in absorption in the Soret region, observed upon steady-state photolysis of a

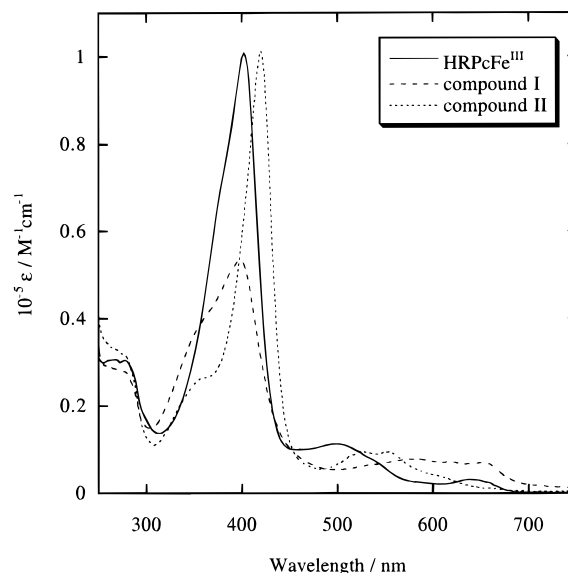
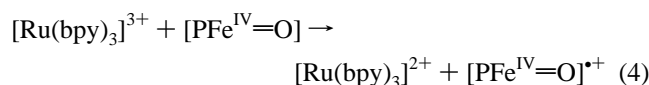
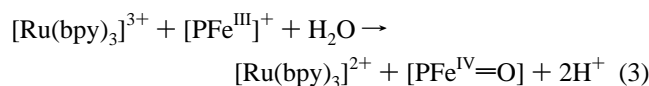
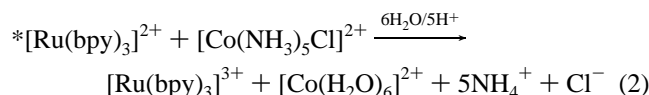
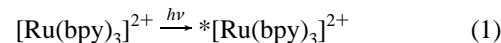


Figure 1. Spectra of $\text{HRPcFe}^{\text{III}}$ and HRPc compound **I** and compound **II**.³² Compound **I** was generated by adding a slight excess of hydrogen peroxide. Compound **I** was reduced to compound **II** by titration with ascorbate until no further increase in absorption at 420 nm was observed. Conditions: $[\text{HRPc}] = 7.0 \mu\text{M}$; $[\text{ascorbate}]_{\text{final}} = 14 \mu\text{M}$; 50 mM borate buffer; pH 9.2.

solution containing $\text{HRPcFe}^{\text{III}}$, $[\text{Ru}(\text{bpy})_3]^{2+}$, and $[\text{Co}(\text{NH}_3)_5\text{Cl}]^{2+}$ (Figure 2a), is consistent with oxidation of the ferric resting state to compound **I**. The steps in the formation of compound **I** are outlined in reactions 1–4.



In the first reaction, the MLCT excited state of $[\text{Ru}(\text{bpy})_3]^{2+}$ is produced by visible irradiation; the excited state is quenched by the Co^{III} complex to generate $[\text{Ru}(\text{bpy})_3]^{3+}$ (reaction 2), and the photogenerated $[\text{Ru}(\text{bpy})_3]^{3+}$ then oxidizes the ferric resting state of the enzyme to compound **II** (reaction 3). In the final step, compound **II** is further oxidized to compound **I** (reaction 4). The clear isosbestic points (Figure 2a) indicate rate-limiting formation of compound **I** followed by fast oxidation to compound **II** without buildup of compound **II**. Subsequent to full photochemical conversion to compound **I**, a new Soret peak at 420 nm is observed (Figure 2b), signaling the formation of compound **II**. Most likely, compound **I** is spontaneously reduced by amino-acid residues in the protein. In alkaline solution, it is possible to obtain complete conversion of the ferric state to compound **II** by this method. In neutral solutions, however, reduction of compound **I** is slower and compound **II** is not as stable, leading to a mixture of compound **I**, compound **II**, and $\text{HRPcFe}^{\text{III}}$. Figure 2b shows that photolysis of compound **II** regenerates compound **I**.

Laser Flash Photolysis. (a) Formation of Compound **II.** In our work on microperoxidase-8, $[\text{Ru}(\text{NH}_3)_6]^{3+}$ was used to

(28) Low, D. W.; Winkler, J. R.; Gray, H. B. *J. Am. Chem. Soc.* **1996**, *118*, 117.

(29) Shannon, L. M.; Kay, E.; Lew, J. Y. *J. Biol. Chem.* **1966**, *241*, 2166.

(30) Ohlsson, P.-I.; Paul, K.-G. *Acta Chem. Scand.* **1976**, *B30*, 373.

(31) Non-commercial program developed to facilitate treatment of data obtained from the laser setup.

(32) It is difficult to obtain quantitative conversion of compound **I** to compound **II**. Taking $\epsilon_{403, \text{HRPcFe}^{\text{III}}} = 1.02 \times 10^5 \text{ M}^{-1} \text{ cm}^{-1}$ and $\epsilon_{420, \text{compound II}} = 1.05 \times 10^5 \text{ M}^{-1} \text{ cm}^{-1}$ (ref 2), we estimate there is 98% conversion to compound **II** based on the spectrum shown in Figure 1.

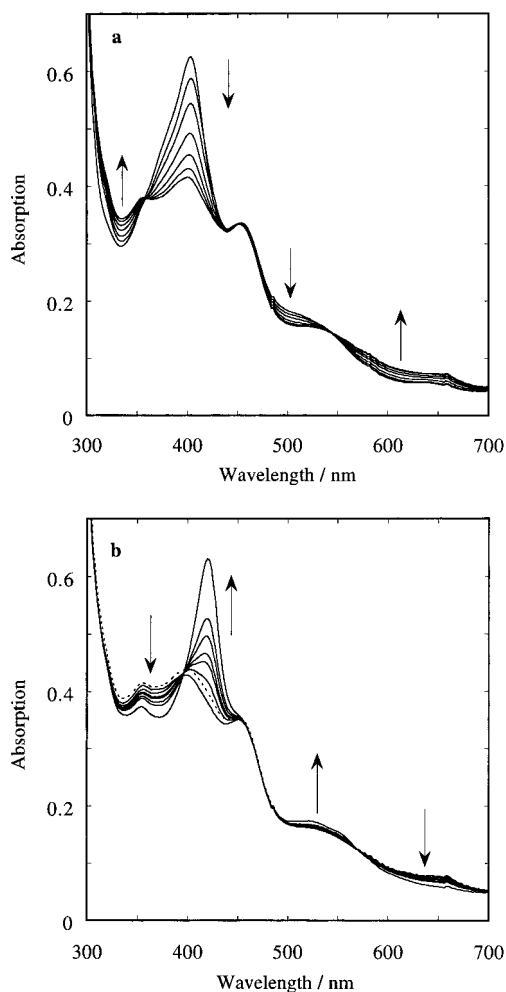


Figure 2. Steady-state photolysis: (a) Oxidation of HRPcFe^{III} to compound **I**; spectra taken at intervals of 30, 60, 90, 120, 180, and 210 s during photolysis. (Note that the isosbestic points at 359 and 544 nm are consistent with the isosbestic points between HRPcFe^{III} and compound **I** in Figure 1; the differences between the spectra in this figure and the spectra in Figure 1 are mainly due to the background absorption of [Ru(bpy)₃]²⁺ ($\lambda_{\text{max}} \sim 450$ nm) and to a smaller extent to absorption from [Co(NH₃)₅Cl]²⁺ (strong absorption below 320 nm).) (b) Reduction of compound **I** to compound **II** in the dark; spectra taken 2, 4, 6, 8, 10, and 18 min after the end of photolysis. (Note that the isosbestic points at 396 and 570 nm are consistent with the isosbestic points between compound **II** and compound **I** in Figure 1.) The dotted spectrum shows the reformation of compound **I** after 1 min of photolysis of compound **II**. Conditions: [HRPcFe^{III}] = 4.9 μ M; [Ru(bpy)₃]²⁺ = 17 μ M; [Co(NH₃)₅Cl]²⁺ = 1 mM; 50 mM borate buffer; pH 9.

quench the excited state of [Ru(bpy)₃]²⁺ (similar to reaction 2).²⁸ We chose to employ [Co(NH₃)₅Cl]²⁺ (reaction 2) for the HRP experiments, since the reduced quencher rapidly aquates; this approach was necessary because the oxidation of HRP is much slower than oxidation of MP8. In blank experiments without enzyme, it was shown that the spontaneous reduction of [Ru(bpy)₃]³⁺ in water³³ was significantly slower than the reaction with the enzyme (reaction 3) under all conditions. However, it was not negligible, especially at pH 10.8, giving rise to small intercepts in the k_{obsd} vs [HRPc] plots. Figure 3 shows typical kinetics traces at 430 and 450 nm from a laser flash photolysis experiment where the [Ru(bpy)₃]²⁺ complex was excited with a 25-ns laser pulse at 480 nm. The kinetics at 430 nm are biphasic; a fast reaction on a millisecond time scale is followed by a much slower reaction (approximately

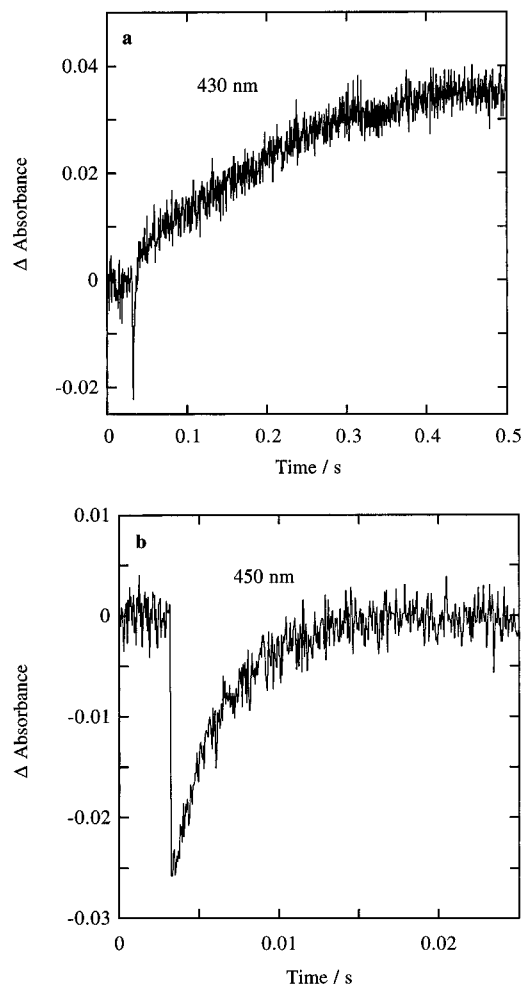


Figure 3. Typical transient kinetics traces at 430 and 450 nm for the photoinduced oxidation of HRPcFe^{III} to compound **II** by [Ru(bpy)₃]³⁺. The trace at 430 nm is biphasic showing the formation of the radical intermediate and the subsequent conversion to compound **II**. The 450-nm trace, at the absorption maximum of [Ru(bpy)₃]²⁺ where the transformation of the protein does not significantly contribute to the spectral changes, is monoexponential, displaying only depletion of [Ru(bpy)₃]³⁺ and buildup of [Ru(bpy)₃]²⁺. Conditions: [HRPcFe^{III}] = 24 μ M; [Ru(bpy)₃]²⁺ = 17 μ M; [Co(NH₃)₅Cl]²⁺ = 5.0 mM; 50 mM borate buffer; pH 8.5.

seconds). In the wavelength region around the 450-nm [Ru(bpy)₃]²⁺ absorption maximum, the transformations of the protein do not significantly contribute to the spectral changes. The traces recorded in this region are therefore monoexponential, displaying only buildup of [Ru(bpy)₃]²⁺ and depletion of [Ru(bpy)₃]³⁺. Kinetics traces were typically recorded in the region 415 < λ < 435 nm and evaluated by a two-exponential fit. The values obtained for the rate constant of the first fast phase agreed well with the values obtained by fitting the 450–460-nm traces to a single exponential function; the depletion of [Ru(bpy)₃]³⁺ thus occurs with the same rate as the initial transformation of the protein. Difference spectra were recorded at 25 and 410 ms after pulsed-laser initiation of the reaction. At these times, each spectrum exhibits absorption from the intermediate formed in the fast phase, as well as absorption of the final product ([Ru(bpy)₃]³⁺ is depleted in less than 25 ms). Using the rate constants for formation of the intermediate (300 s⁻¹) and the conversion of this species to the final product (4.1 s⁻¹) determined from single-wavelength kinetics, it was possible to estimate the composition of the sample at both 25 and 410 ms. With this estimate, the corrected difference spectra between the pure intermediate and the trivalent resting state (spectrum

(33) Ghosh, P. K.; Brunschwig, B. S.; Chou, M.; Creutz, C.; Sutin, N. *J. Am. Chem. Soc.* **1984**, *102*, 4772.

T) and between the pure final product and the trivalent resting state (spectrum L) (Figure 4a) could be simulated.³⁴ As shown in Figure 4a, the difference spectrum between the final product and $[\text{PFe}^{\text{III}}]^+$ (spectrum L) is quite similar to the difference spectrum between compound **II** and the trivalent resting state (spectrum S) calculated from the spectra of compound **II** and $[\text{PFe}^{\text{III}}]^+$ (Figure 1), indicating that compound **II** is the final product in the laser flash experiment. Although the qualitative features of the difference spectrum between the intermediate and $[\text{PFe}^{\text{III}}]^+$ (spectrum T) are somewhat similar to the difference spectrum between $[\text{PFe}^{\text{IV}}=\text{O}]^+$ and $[\text{PFe}^{\text{III}}]^+$ (spectrum L), a more pronounced bleach in the 380–400 nm wavelength region is apparent from the scaled spectra³⁵ in the inset of Figure 4a. Under the assumption that the photochemically generated $[\text{Ru}(\text{bpy})_3]^{3+}$ produced a stoichiometric amount of compound **II**, molar absorbance spectra for photochemically generated intermediate and compound **II** could be calculated (Figure 4b).³⁶ The spectrum of the intermediate shows a broader and less intense Soret peak than the spectrum of the trivalent resting state, which is qualitatively very similar to spectra reported for high-spin iron(III) porphyrin model complexes.²¹ The observed Soret absorption confirms that the intermediate detected in the photochemically driven oxidation of HRPc is a π -cation porphyrin radical, $[\text{PFe}^{\text{III}}]^{\cdot 2+}$.³⁷

Both an X-ray crystal structure analysis³⁸ and molecular dynamics simulations³⁹ show that the HRP heme iron is five-coordinate under physiological conditions. In this structure, the binding site on the distal side of the cavity is open for coordination. It is somewhat surprising that one of the water molecules close to the iron in the heme cavity does not occupy this site in the resting state; however, ferric HRPc undergoes an alkaline transition ($\text{p}K_{\text{a}} = 10.9$) in which the heme iron changes from a five-coordinate, high-spin species to a six-coordinate, low-spin form.^{40,41} Although it has not been

(34) The corrected difference spectra (spectra T and L, Figure 4a) were calculated using the following expressions:

$$\text{intermediate (T): } A_{\text{corrected}} = \frac{(A_{25\text{ms}} - A_{410\text{ms}}\{\text{CII}_{25\text{ms}}/\text{CII}_{410\text{ms}}\}) / (1 - \text{CII}_{25\text{ms}}/\text{CII}_{410\text{ms}})}{A_{410\text{ms}} - A_{25\text{ms}}\{\text{Int}_{410\text{ms}}/\text{Int}_{25\text{ms}}\}} / (1 - \text{Int}_{410\text{ms}}/\text{Int}_{25\text{ms}})$$

$$\text{final product (L): } A_{\text{corrected}} = \frac{(A_{410\text{ms}} - A_{25\text{ms}}\{\text{Int}_{410\text{ms}}/\text{Int}_{25\text{ms}}\}) / (1 - \text{Int}_{410\text{ms}}/\text{Int}_{25\text{ms}})}{A_{25\text{ms}} - A_{410\text{ms}}\{\text{CII}_{25\text{ms}}/\text{CII}_{410\text{ms}}\}} / (1 - \text{CII}_{25\text{ms}}/\text{CII}_{410\text{ms}})$$

$A_{25\text{ms}}$ and $A_{410\text{ms}}$ denote the experimental difference spectra obtained at 25 and 410 ms, respectively; $\text{CII}_{25\text{ms}}$ and $\text{CII}_{410\text{ms}}$ are the calculated fractions of compound **II** at 25 and 410 ms, respectively; and $\text{Int}_{25\text{ms}}$ and $\text{Int}_{410\text{ms}}$ are the calculated fractions of the intermediate at 25 and 410 ms, respectively. The fractions of compound **II** and the intermediate were calculated by use of rate constants for formation of the intermediate (300 s^{-1}) and conversion of the intermediate into the final product (4.1 s^{-1}).

(35) The scaling was done by multiplying the T spectrum (Figure 4a) by a factor that gives the same absorption at 422 nm as the L spectrum.

(36) The difference in extinction coefficient between compound **II** and $\text{HRPcFe}^{\text{III}}$ at 423 nm is $\Delta\epsilon_{423} = 60264 \text{ M}^{-1} \text{ cm}^{-1}$ (Figure 1). Under the assumption that the photochemically generated $[\text{Ru}(\text{bpy})_3]^{3+}$ produced a stoichiometric amount of compound **II**, the ΔOD_{423} of 0.151 measured in spectrum L in Figure 4a then corresponds to conversion of $2.51 \mu\text{M}$ $\text{HRPcFe}^{\text{III}}$ in that particular experiment. Molar absorbance spectra for photochemically generated intermediate and compound **II** could then be calculated by adding an absorption corresponding to $2.51 \mu\text{M}$ $\text{HRPcFe}^{\text{III}}$ (Figure 1) to the corrected spectra in Figure 4a (intermediate spectrum = difference spectrum T + $\text{HRPcFe}^{\text{III}}$ spectrum; compound **II** spectrum = difference spectrum L + $\text{HRPcFe}^{\text{III}}$ spectrum).

(37) There is a possibility that some fraction of the Ru(III) does not oxidize the porphyrin ring but rather another group of the enzyme, for example, a tyrosine residue. This oxidation would not be detectable in the Soret spectrum of the enzyme, since tyrosine radicals do not absorb strongly in this wavelength region. In this case, a smaller absorptivity would be calculated for the π -cation porphyrin radical (Figure 4b).

(38) Gajhede, M. Private communication.

(39) Banci, L.; Carloni, P.; Savellini, G. *Biochemistry* **1994**, *33*, 12356.

(40) Sitter, A. J.; Shifflett, J. R.; Turner, J. *J. Biol. Chem.* **1988**, *263*, 13032 and references therein.

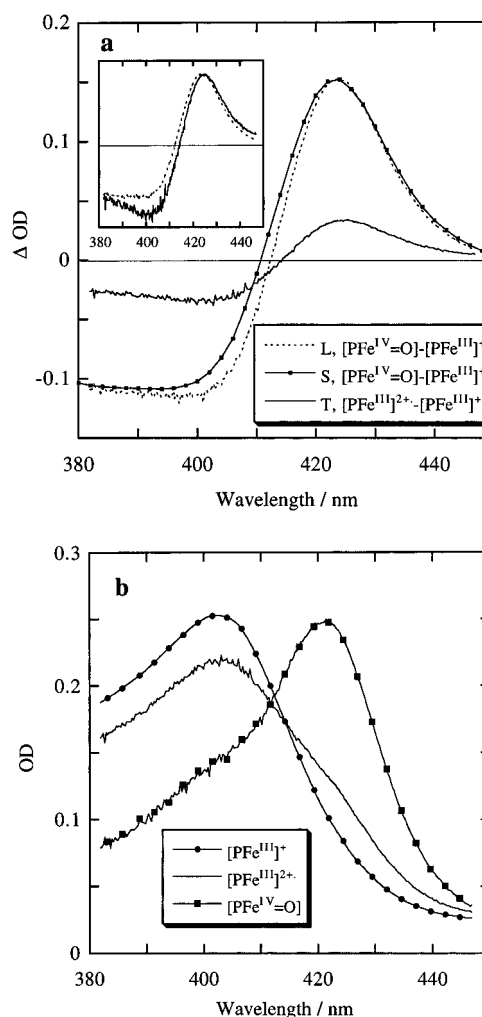


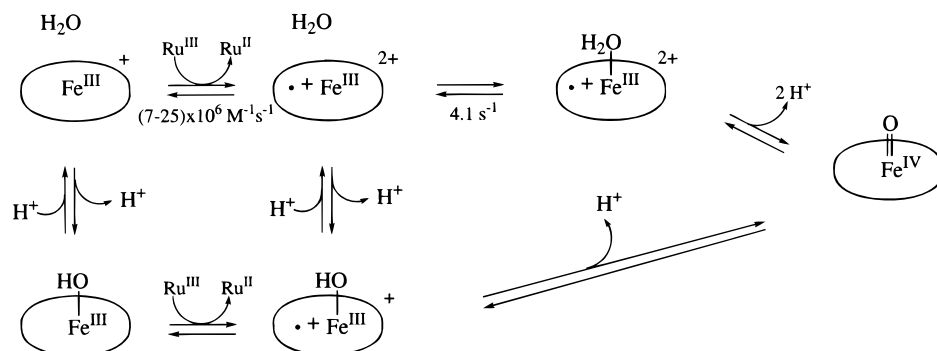
Figure 4. Spectral characterization of the species formed in the photoinduced oxidation of $\text{HRPcFe}^{\text{III}}$. (a) Difference spectra: The transient difference spectrum, T, between the intermediate π -cation porphyrin radical ($[\text{PFe}^{\text{III}}]^{\cdot 2+}$) and $\text{HRPcFe}^{\text{III}}$ ($[\text{PFe}^{\text{III}}]^+$), and the final difference spectrum, L, between compound **II** ($[\text{PFe}^{\text{IV}}=\text{O}]$) and $\text{HRPcFe}^{\text{III}}$ ($[\text{PFe}^{\text{III}}]^+$) were calculated from experimental spectra collected 25 and 410 ms after the laser pulse. Conditions: $[\text{HRPcFe}^{\text{III}}] = 14 \mu\text{M}$; $[\text{Ru}(\text{bpy})_3]^{3+} = 17 \mu\text{M}$; $[\text{Co}(\text{NH}_3)_5\text{Cl}^{2+}] = 5.0 \text{ mM}$; 50 mM borate buffer; $\text{pH} 9.75$. The steady-state spectrum, S, between compound **II** ($[\text{PFe}^{\text{IV}}=\text{O}]$) and $\text{HRPcFe}^{\text{III}}$ ($[\text{PFe}^{\text{III}}]^+$) was calculated and scaled from the spectra in Figure 1 (the scaling involved multiplying the compound **II**– $\text{HRPcFe}^{\text{III}}$ difference spectrum (Figure 1) by a factor that gave the best qualitative agreement with spectrum S). Inset: Scaled difference spectra³⁵ between $[\text{PFe}^{\text{III}}]^{\cdot 2+}$ and $[\text{PFe}^{\text{III}}]^+$ and between $[\text{PFe}^{\text{IV}}=\text{O}]$ and $[\text{PFe}^{\text{III}}]^+$. (b) Absolute spectra: The spectra for $[\text{PFe}^{\text{III}}]^{\cdot 2+}$ and $[\text{PFe}^{\text{IV}}=\text{O}]$ were calculated from the spectra in Figure 4a and the known spectra for compound **II** and the trivalent resting state (Figure 1) under the assumption that photochemically generated $[\text{Ru}(\text{bpy})_3]^{3+}$ produces a stoichiometric amount of compound **II**.³⁶

established with certainty whether this transition is associated with coordination of an amino-acid residue (for example, the distal histidine) or hydroxide, hydroxide coordination is supported by resonance Raman experiments.⁴⁰

The proposed mechanism for oxidation of $\text{HRPcFe}^{\text{III}}$ to compound **II** is outlined in Scheme I. In the pH region $7.8 < \text{pH} < 9.8$, where the heme iron is five-coordinate (upper path), the fast reaction (Figure 3) is linearly dependent on the concentration of HRPc under pseudo-first-order conditions with enzyme in excess (Figure 5a). The rate of the slower reaction, however, is independent of the concentration of HRPc (Figure

(41) Harbury, H. A. *J. Biol. Chem.* **1957**, *225*, 1009.

Scheme 1. Oxidation of HRPcFe^{III} to Compound **II** by Photochemically Generated [Ru(bpy)₃]³⁺ via the Formation of a π -Cation Porphyrin Radical Intermediate^a



^a The indicated rate constants are for the forward reactions.

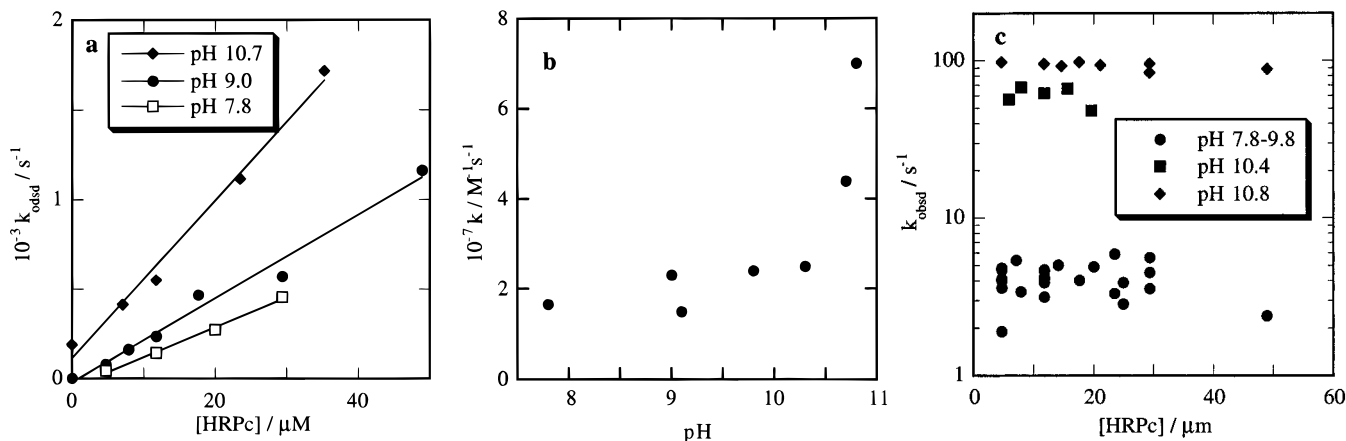


Figure 5. Kinetics of the oxidation of HRPcFe^{III} to compound **II**: (a) Dependence of the rate of formation of the π -cation porphyrin radical on [HRPc]. (b) Dependence of the rate of formation of the π -cation porphyrin radical on pH. (c) Dependence of the rate of conversion of the π -cation porphyrin radical intermediate to compound **II** on [HRPc] and pH. Conditions: [Ru(bpy)₃]²⁺ = 17 μ M; [Co(NH₃)₅Cl²⁺] = 5.0 mM; ambient temperature (\sim 22 $^{\circ}$ C); pH was adjusted using either phosphate (pH 7.0–7.8), borate (pH 8.5–9.8), or carbonate (pH 10.3–10.8); the concentration of buffer was between 10 and 100 mM.

5c). The experimental rate laws for the two reactions, eqs 5 and 6, are therefore consistent with the proposed mechanism.

$$-d[\text{PFe}^{\text{III}}]^+/dt = (k_{\text{blank}} + k_{3a}[\text{PFe}^{\text{III}}]^+)[\text{Ru}(\text{bpy})_3]^{3+} \quad (5)$$

$$d[\text{PFe}^{\text{IV}}=\text{O}]/dt = k_{3b}[\text{PFe}^{\text{III}}]^{\bullet 2+} \quad (6)$$

In eq 5, k_{blank} represents the observed rate constant for the spontaneous first-order decay of [Ru(bpy)₃]³⁺ in the absence of enzyme, giving rise to small intercepts in Figure 5a. In eqs 5 and 6, k_{3a} and k_{3b} are the rate constants for the second-order formation of the radical and the first-order conversion to compound **II**, respectively, the steps in reaction 3. There is no pH dependence for the transformation of the radical into compound **II** in the region 7.8 < pH < 9.8 (Figure 5c) and, therefore, either binding of a water molecule or the subsequent electron-transfer step can be rate limiting for compound **II** formation. In our previous study using MP8,²⁸ where the resting state heme iron coordinates a hydroxide ligand in the sixth position, we could not observe the π -cation porphyrin radical intermediate (unless we trapped it at lower pH) because the conversion to compound **II** is too fast; this is also what happens in the present system in the pH region in which the heme iron coordinates a hydroxide ligand (*vide infra*). Based on these findings, then, we suggest that the rate-limiting step for the transformation of the porphyrin radical intermediate is water coordination, and that the subsequent proton/electron transfer steps are fast.⁴²

In the pH region 10.3 < pH < 10.8, where there is an equilibrium mixture of five- and six-coordinate hemes (at pH 10.8, \sim 40% of the heme iron is hydroxide ligated and the rest is still five-coordinate iron), we observe a mixture of compound **II** and the radical intermediate after the fast kinetics phase. The observations in this pH region can be rationalized if the rate-limiting step for the generation of compound **II** in six-coordinate HRPc is formation of the radical intermediate, and the subsequent proton/electron-transfer step is fast enough to give only a negligible steady-state concentration of the π -cation porphyrin radical as found for six-coordinate MP8 at high pH.²⁸ There will, therefore, be a burst of compound **II** formation from the enzyme molecules that initially contain hydroxo-ligated heme. Since the enzyme molecules that have five-coordinate hemes will still generate the five-coordinate radical intermediate, there will be a mixture of compound **II** and π -cation radicals after the end of the first kinetics phase. The increase in the rate of porphyrin radical formation at pH > 10.3 (Figure 5b) is most likely attributable to a higher driving force for porphyrin oxidation in the six-coordinate ferric state of the enzyme.⁴³

The slower kinetics phase in the pH region 10.3 < pH < 10.8 is the rate-limiting step for conversion of the five-coordinate radical intermediate to compound **II**. It is interesting that the observed rate constant at pH 10.8 ($95 \pm 7 \text{ s}^{-1}$) is over 20 times

(42) It is interesting to note that binding of H₂O to five-coordinate Fe^{II} myoglobin takes place with a first-order rate constant of 0.5 s⁻¹, which puts this reaction on the same timescale as HRPc ferryl formation at pH < 9.8. King, B. C.; Hawkrige, F. M.; Hoffman, B. M. *J. Am. Chem. Soc.* **1992**, *114*, 10603.

larger than that at lower pH ($4.1 \pm 0.9 \text{ s}^{-1}$). At high pH, a more facile pathway than binding of H_2O , namely, one involving coordination of OH^- to the radical intermediate (Scheme 1), is available for formation of compound **II**.⁴⁴ Importantly, in connection with the ongoing discussion of the structure of alkaline HRP,⁴⁰ we emphasize that our findings favor a heme structure involving coordination of a hydroxide ligand in the sixth position of the heme iron. Indeed, it would be difficult to reconcile the observed pH effect on the rate of ferryl formation in terms of amino-acid coordination.

In summary, our kinetics data support Scheme 1. Under conditions where the heme iron is five-coordinate (upper path), the ferryl oxygen is derived from an uncoordinated water molecule. This water molecule binds to the radical intermediate formed by oxidation by $[\text{Ru}(\text{bpy})_3]^{3+}$. In subsequent steps, proton and intramolecular electron transfers generate the ferryl form of the enzyme. In more alkaline solutions (lower path), where the heme iron is six-coordinate, a hydroxo-ligated ferric π -cation porphyrin radical intermediate is formed prior to the generation of compound **II**.

(b) Formation of Compound I. The photoinduced oxidation of compound **II** to compound **I** (reactions 1–2 and 4) was studied as described above for oxidation of $\text{HRPcFe}^{\text{III}}$ to compound **II**. Compound **II** was generated by steady-state photolysis of a ferric HRPc solution to form compound **I**, according to reactions 1–4, followed by spontaneous reduction of compound **I** to compound **II** (as shown in Figure 2). The difference spectrum (Figure 6a) taken at the end of the reaction is in good agreement with a hydrogen peroxide generated difference spectrum between compound **I** and compound **II** (Figure 6a). The observed rate constant for formation of compound **I** increases linearly with the concentration of excess compound **II** and there is only a negligible difference in the pH 10.3 ($k_7 = 1.1 \times 10^8 \text{ M}^{-1} \text{ s}^{-1}$) and the pH 10.8 ($k_7 = 1.2 \times 10^8 \text{ M}^{-1} \text{ s}^{-1}$) rate constants (Figure 6b), indicating a simple rate law (eq 7):⁴⁵



At pH 10.3, the oxidation of compound **II** to compound **I** is slightly faster than oxidation of $\text{HRPcFe}^{\text{III}}$ to the radical intermediate,⁴⁶ but compound **II** to compound **I** conversion is much faster than the oxidation of $\text{HRPcFe}^{\text{III}}$ to compound **II** below pH 9.8, consistent with previous results for oxidation of HRP by K_2IrCl_6 .¹⁰ The fact that the porphyrin-centered

(43) There is a large difference in the reactivities of HRPc and MP8 with $[\text{Ru}(\text{bpy})_3]^{3+}$; specifically, $\text{MP8Fe}^{\text{III}}$ is oxidized 200 times faster than $\text{HRPcFe}^{\text{III}}$ to form the porphyrin radical intermediate.²⁸ In HRP, the heme is buried in the protein matrix with only the heme edge exposed to solvent. In contrast, the heme in MP8 should be readily accessible to $[\text{Ru}(\text{bpy})_3]^{3+}$, which is the probable reason that its oxidation is so much faster.

(44) It was not possible to run experiments above pH 10.8, since both the Ru sensitizer and the Co quencher are not stable in strongly alkaline solution.

(45) A second, slower reaction, with <10% of the amplitude of the main reaction, also was observed. The final difference spectrum had the same qualitative features as the difference spectrum between compound **I** and compound **II** of HRP.

(46) It should be emphasized that a heterogenous mixture is obtained after consecutive laser shots on a freshly prepared solution containing the enzyme in its resting state. As soon as compound **II** is formed (reactions 1–3), it will compete with $\text{HRPcFe}^{\text{III}}$ for $[\text{Ru}(\text{bpy})_3]^{3+}$ (reactions 3 and 4). Since reaction 4 is somewhat faster than formation of the radical intermediate, it will account for an increasing percentage of $[\text{Ru}(\text{bpy})_3]^{3+}$ depletion as the concentration of compound **II** builds up.

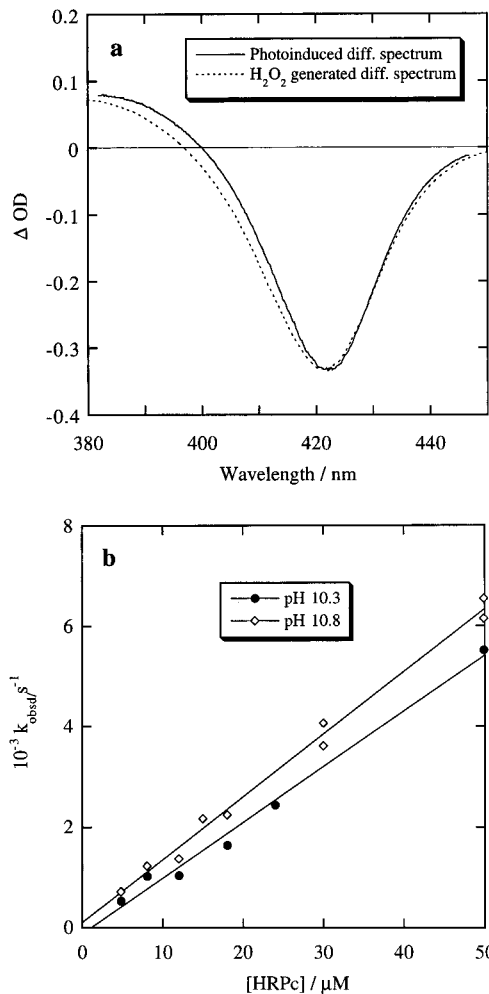


Figure 6. Spectral changes and kinetics for oxidation of compound **II** to compound **I**: (a) Comparison of the difference spectra between compound **I** and compound **II** generated by photoinduced oxidation and by oxidation by hydrogen peroxide.⁴⁵ The spectrum of the photogenerated compound **I** was collected 25 ms after initiation of the reaction with a laser pulse. Conditions: $[\text{HRPcFe}^{\text{III}}] = 14 \mu\text{M}$; $[\text{Ru}(\text{bpy})_3^{2+}] = 17 \mu\text{M}$; $[\text{Co}(\text{NH}_3)_5\text{Cl}_2^{2+}] = 5.0 \text{ mM}$; 50 mM borate buffer; pH 9.75. The hydrogen peroxide generated difference spectrum was calculated from the spectra in Figure 1. (b) Dependence of the rate of oxidation of compound **II** to compound **I** on $[\text{HRPc}]$ and pH. Conditions: $[\text{Ru}(\text{bpy})_3^{2+}] = 17 \mu\text{M}$; $[\text{Co}(\text{NH}_3)_5\text{Cl}_2^{2+}] = 5.0 \text{ mM}$; 50 mM carbonate buffer; ambient temperature ($\sim 22 \text{ }^\circ\text{C}$).

oxidation of $\text{HRPcFe}^{\text{III}}$ to the π -cation radical and the oxidation of compound **II** to compound **I** occur on the same time scale is easily rationalized by the similarity of the two reactions. The oxidation of the five-coordinate ferric resting state to compound **II**, however, involves both binding of a water molecule and coupled proton and electron transfer. This conversion, of course, is a more complex process than a simple electron transfer involving only the porphyrin ring.

Acknowledgment. We thank Pat Farmer, Michael Gajhede, Don Low, and Tom Poulos for helpful discussions. Postdoctoral fellowships from the Swedish Natural Science Research Council (J.B., T.P.) and from the Swedish Institute and the Wenner-Gren Center Foundation (J.B.) are gratefully acknowledged. This work was supported by the National Science Foundation.